Research on Chemical Intermediates
https://doi.org/10.1007/s11164-020-04323-4

A spectroscopic insight into the interaction of chromene 1,2,4-oxadiazole-based compounds with bovine serum albumin

Nilima Priyadarsini Mishra[1] · Lakoji Satish[1] · Seetaram Mohapatra[1] · Sabita Nayak[1] · Harekrushna Sahoo[2]

Received: 6 August 2020 / Accepted: 9 November 2020

Abstract

Four synthesized 2*H*-chromene-based 1,2,4-oxadiazole compounds (**6a-6d**) were studied for binding with bovine serum albumin (BSA) by different spectroscopic and thermodynamic analyses. A molecular docking program was used to find out the possible binding sites and binding affinity of 2*H*-chromene based 1,2,4-oxadiazole compounds with bovine serum albumin (BSA). The intrinsic fluorescence of BSA was quenched by these compounds through static quenching mechanism, and the estimated binding constant (K_b) value was found to be 1.5×10^3–10×10^3. The conformational changes of BSA were monitored by circular dichroism analysis, and it was observed that BSA is structurally stable in the presence of these compounds. The thermodynamic results indicated that the interaction process is spontaneous and the binding between oxadiazole compounds and BSA is mainly driven by hydrogen bonding and van der Waals forces. This study would be helpful to understand the biological benefits of oxadiazole-based compounds as well as the nature of interactions with biomolecules.

Electronic supplementary material The online version of this article (https://doi.org/10.1007/s11164-020-04323-4) contains supplementary material, which is available to authorized users.

✉ Seetaram Mohapatra
seetaram.mohapatra@gmail.com

[1] Department of Chemistry, Ravenshaw University, Cuttack 753003, India

[2] Department of Chemistry, NIT Rourkela, Rourkela 769008, India

Published online: 17 November 2020

Graphic abstract

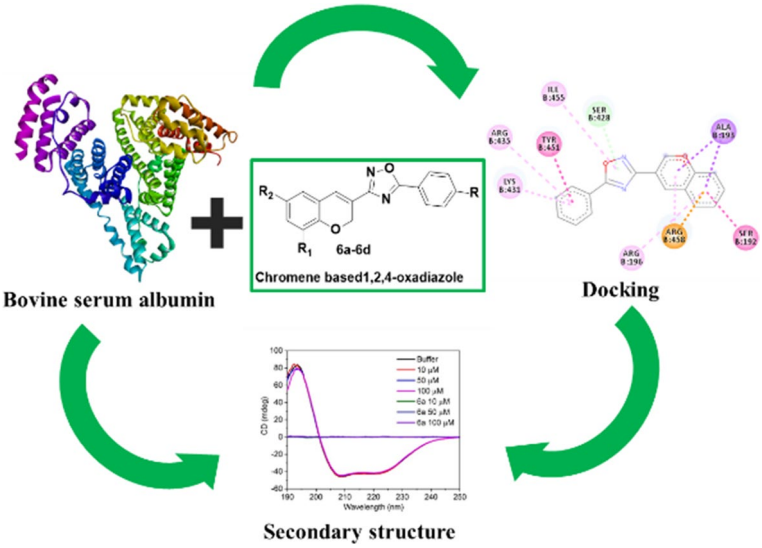

Keywords 1,2,4-oxadiazole · Microwave irradiation · Bovine serum albumin · Molecular docking · Circular dichroism

Introduction

Heterocyclic molecules implanted with nitrogen and oxygen atoms have been used in diverse biological and pharmacological applications [1]. Among different types of nitrogen- and oxygen-containing heterocyclic compounds, five-membered heterocyclic compounds including azole, thiazole, oxadiazole, triazene, imidazole, purines, pyrazole, etc., play a very important role in human life due to their medicinal action against several diseases [2–9]. Specifically, oxadiazole-based compounds were found to exhibit anti-inflammatory, antimicrobial, antitubercular, antidepressant, antimalarial, anti-HIV and anticancer properties [10–19]. Due to their biological activities, synthesis of novel oxadiazole compounds is the current research area of interest to produce analgesics, antispasmodics and anti-inflammatories. Recently, our research group reported microwave-assisted synthesis of chromene-based 1,2,4-oxadiazole molecules having potent antibacterial activity [20]. Also, as reported earlier, these oxadiazole nuclei contribute significant bioactivity due to their lipophilic nature and have ability to bind with the target protein through hydrogen bonding [21].

Protein molecules play a crucial role in effective action of several drugs in living beings [22]. The pharmacodynamics and pharmacokinetics of drugs generally depend on the binding of these molecules with albumin proteins [23–25]. Therefore, studying the binding mechanism responsible for the molecular interactions between drug molecules and albumin could be helpful in designing new bioactive

molecules. We selected bovine serum albumin (BSA) as a model protein for this study as it is largely present in the blood plasma and plays a vital role in the transportation of several endogenous and exogenous ligands (such as fatty acids, amino acids, steroids, and various drugs) [26]. Also, BSA is structurally similar (around 76%) to human serum albumin (HSA). It consists of 583 amino acid residues with a molecular weight of 66 kDa. BSA structure can be divided into three domains (I, II and III), and each domain further contains two subdomains (A and B).

There were only few reports on interaction studies of oxadiazole compounds with biomolecules that are described here. Laskar, K et al. reported the synthesis of 1,3,4-oxadiazole compounds of fatty acids and evaluated the binding interaction of (Z)-(2)-(heptadec-8′-enyl)-5-methyl-1,3,4-oxadiazole with serum albumin using different spectrometers [27]. In another study by Anouar, E H et al. several indole-based oxadiazole compounds were synthesized and screened for their inhibitory potential against *β*-glucuronidase [28]. Also, they used molecular docking to find the interactions between these compounds and the active binding site. Santosh, R et al. investigated the docking of several oxadiazole compounds with DNA and performed binding studies using UV–Vis spectrometer [29].

In this study, we designed and synthesized four different 2*H*-chromene-based 1,2,4-oxadiazole compounds (Fig. 1). The main aim of our work is to understand the binding mechanism involved in the interaction between the synthesized oxadiazole compounds and BSA. For that, we opted a universal strategy combining both experimental and molecular docking methods. Different spectrophotometric methods were employed to understand molecular-level interactions and the effect of oxadiazole compounds on the structure and stability of BSA. Also, we used AutoDock Vina program to find out the possible binding sites as well as the binding affinity between the oxadiazole compounds and BSA. This combining approach will be helpful to study several protein-drug systems.

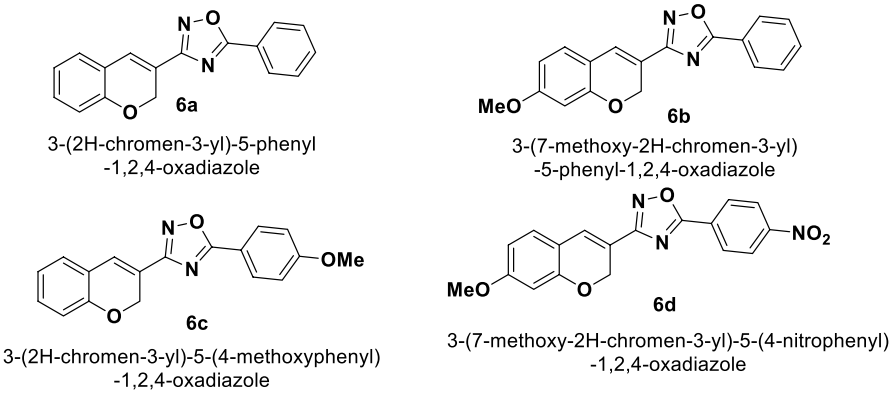

Fig. 1 1,2,4-oxadiazole compounds synthesized in this work. **a** 3-(2*H*-chromen-3-yl)-5-phenyl-1,2,4-oxadiazole, **b** 3-(7-methoxy-2*H*-chromen-3-yl)-5-phenyl-1,2,4-oxadiazole, **c** 3-(2*H*-chromen-3-yl)-5-(4-methoxyphenyl)-1,2,4-oxadiazole and **d** 3-(7-methoxy-2*H*-chromen-3-yl)-5-(4-nitrophenyl)-1,2,4-oxadiazole

Experimental

Materials

BSA (Product No.- A2153) was purchased from Sigma-Aldrich and was used without any further purification. All samples are prepared using PBS buffer (0.01 M). Milli-Q water (18 M cm, Millipore, Bedford, MA) was used to prepare PBS buffer. The 2*H*-chromene-based 1,2,4-oxadiazole compounds (**6a-6d)** were synthesized in our laboratory and purified by recrystallization method [20]. For synthesizing these 1,2,4-oxadiazole compounds, all reagents and solvents were purchased from commercial suppliers. Salicylaldehyde, acrylonitrile, DABCO, Et_3N, hydroxylamine hydrochloride, EDCI, HOBT and benzoic acids were purchased from Sigma-Aldrich. The progress of the reaction was monitored by TLC on silica gel 60 F_{245}-coated TLC plates (Merck KGaA, Darmstadt, Germany).

Methods

Molecular docking

AutoDock Vina 1.5.4 program was used for the blind molecular docking between BSA and oxadiazole compounds. The crystal structure of BSA (PDB-3v03) and optimized chemical structure of chromene-based 1,2,4-oxadiazole compounds prepared by ChemDraw ultra 8 were used in the docking. Polar hydrogens and partial atomic Kollman charges were assigned to BSA using the default settings in auto-dock tools. The center of the grid and grid dimension was set at (90.398 × 28.894 × 23.482) Å and (84 × 56 × 82) Å, respectively. Out of the nine conformations produced, the lowest energy conformation was taken to analyze the results. Discovery Studio visualizer software was used for visualization of the binding site residues.

Sample preparation for interaction studies

A stock solution of oxadiazole compounds was prepared by dissolving the required amount of the compound in PBS buffer containing 1% ethanol. BSA–oxadiazole solutions for the spectroscopic studies were prepared by adding a fixed amount of stock oxadiazole solution to the protein solution to obtain final desired concentration of compound. (The details of oxadiazole compound and BSA concentrations were given in the respective section.) After addition of the compound, the solutions were sonicated followed by incubation at room temperature for 2 h to attain equilibrium.

Fluorescence spectral measurements

The fluorescence measurements were carried out with a Horiba Jvon Spectrometer (Fluoromax-4P). The fluorescence was collected as a function of wavelength

in the range of 305–450 nm. Excitation and emission slit widths were fixed at 5 nm for each. The protein concentration was fixed at 2 μM, and oxadiazole compounds concentration was varied from 0 to 100 μM.

The fluorescence intensities are corrected for absorption of the exciting light and/or reabsorption of the emitted light by the molecules present in the solution to eliminate the inner filter effect using the relationship

$$I_{cor} = I_{obs} e^{(A_{ex}+A_{em})/2}$$

where I_{cor} and I_{obs} are the corrected and observed fluorescence intensities, respectively. A_{ex} and A_{em} are the absorption values of oxadiazole compounds at the excitation and emission wavelengths, respectively.

Absorption measurements

The absorption spectra were performed on Cary-100UV-Vis spectrophotometer, and 1.0 cm quartz cells are used for the measurements. The concentration of BSA was 2 μM, and oxadiazole compounds were varied from 0 to 100 μM.

Circular dichroism spectroscopy

The CD spectra were obtained using a JASCO spectropolarimeter equipped with a thermostat-controlled cell holder. The protein concentration was 2 μM, and oxadiazole concentration was varied from 0 to 100 μM. The far-UV region was scanned between 200 and 260 nm with an average of three scans and a bandwidth of 1 nm.

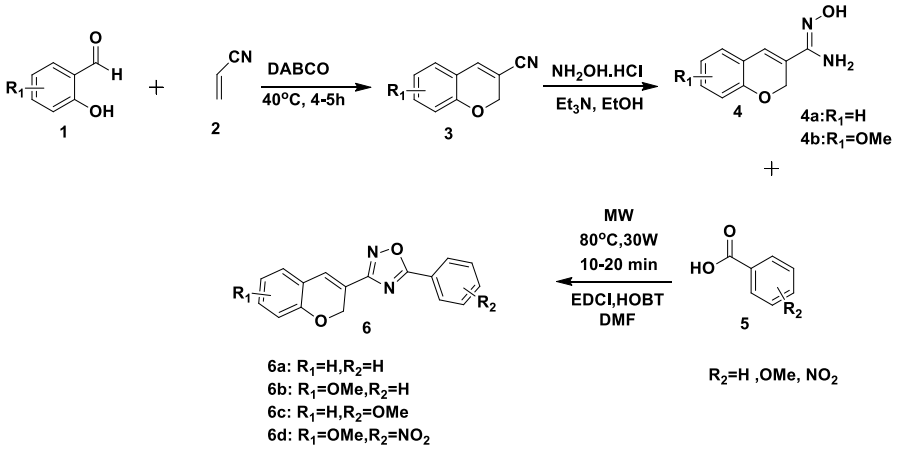

Scheme 1. Synthesis of 1,2,4-Oxadiazole-based compounds **6a**, **6b**, **6c**, **6d**

Synthesis of 1,2,4-oxadiazole-based compounds

The synthesis of chromene-based 1,2,4-oxadiazole compounds **6(a-d)** was described in our previous report [20]. In Scheme 1, substituted chromene-3-carbonitriles **3(a-b)** were prepared by following one-pot two-component method by using salicylaldehyde **1(a-b)** and acrylonitrile **2(a-b)** in the presence of DABCO as catalyst under solvent-free condition at room temperature in good to high yield. After that, chromene-3-carbonitriles **3(a-b)** were treated with hydroxylamine hydrochloride using Et_3N in ethanol for 2 h at 40 °C to obtain N-hydroxy-2*H* chromene-3-carboximidamide **4(a-b)** in to excellent yield. For the synthesis of chromene-based 1,2,4-oxadiazole compounds **6(a-d),** *N*-hydroxy-2*H* chromene-3-carboximidamide **4**(**a-b**) and substituted benzoic acid **5** reacted in the presence of EDCI/HOBT in DMF under microwave irradiation at 80 °C, 30 wt for 20 min to produce good to excellent yield. The product **6(a-d)** was purified by using column chromatography with 92%, 90%, 85%, 80% of yield, respectively. The structures of the synthesized chromene-based 1,2,4-oxadiazole compounds **6(a-d)** were confirmed by ^{1}H NMR, C^{13} NMR and by mass spectroscopy.

3-(2H-chromen-3-yl)-5-phenyl-1,2,4-oxadiazole (6a). Yellowish-white solid; (92%). m.p. 118–120 °C; 1 H-NMR(400 MHz, CDCl 3) δ (ppm): 8.17 (d, J =8.0 Hz, 2 H, Ar-H), 7.63–7.52 (m, 4 H, Ar-H), 7.25–7.18 (m, 2 H, Ar-H), 6.94–6.87 (m, 2 H, Ar-H), 5.25 (s, 2 H, CH 2); 13 C-NMR (100 MHz, CDCl 3): δ 175.3, 166.4, 154.7, 133.0, 131.1, 129.2, 128.4, 128.3, 124.1, 121.9, 121.5, 119.5, 116.2, 64.6; ESIHRMS (m/z): Anal . Calcd for C 17 H 12 N 2 O 2 [M+H] + 277.0899; found: 277.0998.

3-(7-methoxy-2H-chromen-3-yl)-5-phenyl-1,2,4-oxadiazole(6b). White solid; (90%) m.p. 203–205 °C; 1 H NMR(CDCl 3 , 400 MH Z) δ (ppm): 8.17 (d, J =8.0 Hz, 2 H, Ar-H), 7.62–7.53 (m, 4 H, Ar-H), 7.11(d, J =8.0 Hz, 1 H, Ar-H), 6.51 (d, J =8.0 Hz, 1 H, Ar-H), 6.47 (d, J =2.0 Hz,1 H, Ar-H), 5.23 (s, 2 H, CH 2), 3.81 (s, 3 H, OMe); C 13 NMR (CDCl 3 , 100 MHz) δ (ppm): 175.0, 166.4,162.1, 156.1, 132.8, 129.2, 129.1, 128.2, 128.1, 124.1, 116.1, 114.7, 108.0, 101.6, 64.7, 55.4; ESI-HRMS (m/z): Anal. Calcd for C 18 H 14 N 2 O 3 [M+H] + 307. 1004 found: 307.1075.

3-(2H-chromen-3-yl)-5-(4-methoxyphenyl)-1,2,4-oxadiazole(6c). White solid; (85%) m.p. 128–130 °C; 1 H-NMR (400 MHz, CDCl3): δ 8.10 (d, J =8 Hz, 2 H, Ar-H), 7.53 (s, 1 H, Ar-H), 7.25–7.16 (m, 2 H, Ar-H), 7.02–7.00 (m, 2 H, Ar-H), 6.93–6.86 (m, 2 H, Ar-H), 5.25 (s, 2 H, CH 2), 3.90 (s, 3 H, OMe); 13 C NMR (100 MHz, CDCl 3): δ 175.2, 166.2, 163.4, 154.7, 131.0, 130.2, 128.3, 128.0, 121.9, 121.5, 119.6, 116.3, 116.1, 114.6, 64.6, 55.6; ESI-HRMS (m/z): Anal . Calcd for C 18 H 14 N 2 O 3 [M+H] + 307.1004; found: 307.1093.

3-(7-methoxy-2H-chromen-3-yl)-5-(4-nitrophenyl)-1,2,4-oxadiazole(6d). Yellow solid; (80%) m.p.140–142 °C, 1 H NMR (CDCl 3 , 400 MHz) δ (ppm): 8.42–8.36

(m, 4 H, Ar-H), 7.55 (s, 1 H, Ar-H), 7.12 (d, J =8.0 Hz, 1 H, Ar-H), 6.52 (dd, J =4 Hz, 8 Hz, 1 H, Ar-H), 6.46 (d, J =4 Hz, 1 H, Ar-H), 5.22 (s, 1 H, CH 2), 3.81 (s, 3 H, OMe).C 13 NMR (CDCl 3 , 100 MHz) δ (ppm): 172.9, 166.8, 162.4, 156.2, 150.2, 129.4, 129.3, 129.2, 128.9, 124.3, 115.4, 114.4, 108.2, 101.7, 64.5, 55.5.

Results and discussion

Molecular docking

To identify the possible binding sites of the oxadiazole molecule on BSA, AutoDock Vina program was used. This enabled us to predict the binding of oxadiazole compounds with BSA. It is noteworthy that all the oxadiazole compounds are bound at the interface between two subdomains IIA and IIIA (Fig. 2 and Fig. S1). The interactive residues of BSA for the oxadiazole molecules are as follows. (i) For 6a, the residues are Arg 458, Ile 455, Tyr 451, Arg 435, Lys 431, Ser 428 (H-bond), Arg 196, Ala 193, Ser 192 (ii) For 6b, the residues are Arg 458 (H-bond), Ile 455, Tyr 451, Arg 435, Lys 431, Ser 428 (H-bond), Ala 193, Ser 192, (iii) For 6c, the residues are Arg 458, Ile 455, Tyr 451, Arg 435, Lys 431, Ser 428 (H-bond), Ala 193, Asp 108, and (iv) For 6d, the residues are Arg 458 (H-bond), Tyr 451, Arg 435, Lys 431, Ser 192 (H-bond), Ala 193, Ser 428 (H-bond), His 145 (H-bond).

The binding free energies for oxadiazole derivatives (**6a**, **6b**, **6c**, and **6d**) were observed to be -9.2, −9.5, −9.7, −10.0 kcal/mol, respectively. Out of the four compounds, 3-(2H-chromen-3-yl)-5-phenyl-1,2,4-oxadiazole (**6a**) exhibited lowest binding and 3-(7-methoxy-2H-chromen-3-yl)-5-(4-nitrophenyl)-1,2,4-oxadiazole (**6d**) exhibited highest binding with BSA. Therefore, we selected these particular compounds for further analysis to understand binding interactions with BSA. For simplicity, we used only abbreviation for these compounds, **6a** (lowest binding) and **6d** (highest binding) in the whole work.

Fluorescence measurements

Intrinsic fluorescence measurements can provide valuable information about the change in structure and the microenvironment in the vicinity of the fluorophores during the interaction of the ligand molecules with the protein. BSA contains three intrinsic fluorophore residues (Trp, Tyr and Phe), out of which Trp has the highest quantum yield and Phe has the lowest quantum yield. There are two Trp residues (Trp 134 and Trp212) in BSA. Trp 134 was present on surface in domain IB, and Trp 212 was present in the hydrophobic pocket of domain IIA [30]. In order to get valuable information about the change in the microenvironment of Trp residues after interaction with oxadiazole derivatives, BSA was excited at 295 nm to avoid fluorescence interference from Tyr and Phe residues. Two important fluorescence parameters, namely maximum intensity (I_{max}) and maximum emission wave length (λ_{max}), were explored for the BSA–oxadiazole systems. Figure 3 shows the fluorescence spectra of BSA in the presence of oxadiazole compounds (**6a** and **6d**) with varying

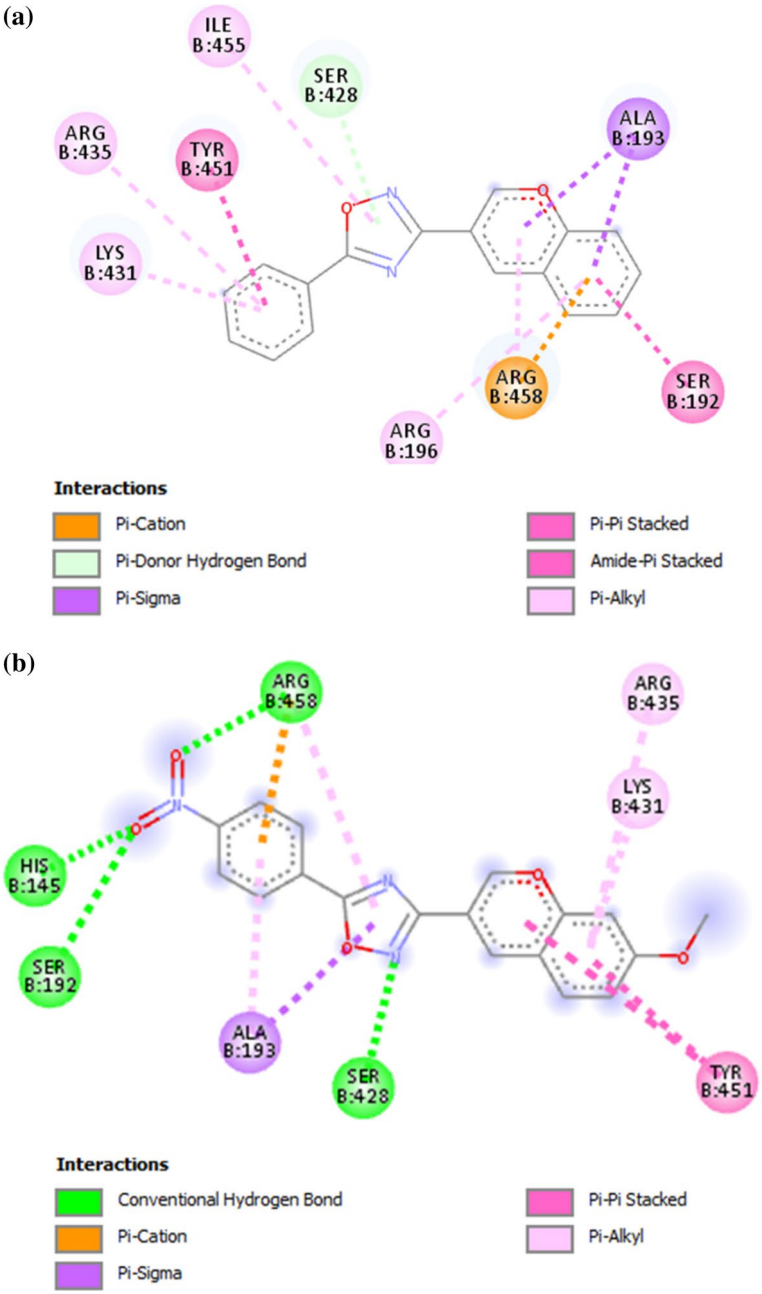

Fig. 2 Molecular docking of 3-(2H-chromen-3-yl)-5-phenyl-1,2,4-oxadiazole (**6a**) (**a**) and 3-(7-methoxy-2H-chromen-3-yl)-5-(4-nitrophenyl)-1,2,4-oxadiazole (**6d**) (**b**) with BSA

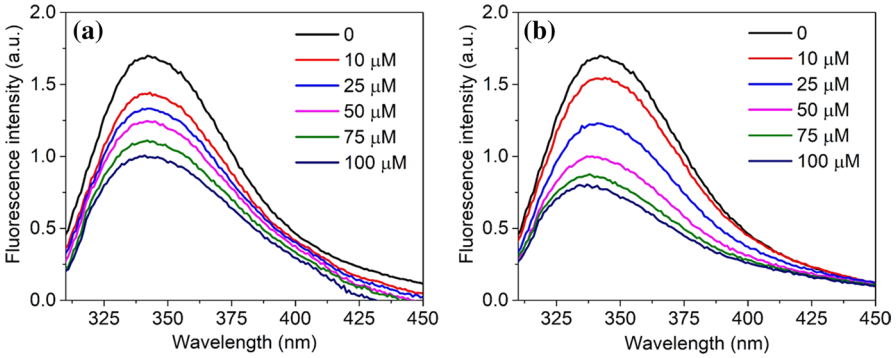

Fig. 3 Representative fluorescence emission spectra of BSA in the absence and presence of oxadiazole compounds with increasing concentrations (0, 10, 25, 50, 75, 100 μM). **a 6a** and **b 6d**

concentration. The fluorescence intensity of BSA decreases gradually with increase in the concentration of oxadiazole derivatives. The λ_{max} of BSA in the buffer solution is observed to be 344 nm. In the presence of oxadiazole compounds, it was observed that there was no change in emission maxima in the case of "**6a**," whereas slight blueshift was noticed in the case of "**6d**" at higher concentration. Any changes in emission maxima generally indicate the change in polarity around the Trp residues. This can be attributed to either (a) internalization of Trp into protein core during protein folding which enhances the hydrophobicity or (b) replacement of polar water molecules from the vicinity of Trp by less polar oxadiazole compounds. In our case, the blueshift of λ_{max} implies a decrease in the polarity and thus an increase in the hydrophobicity in the microenvironment of the Trp residues. Since the oxadiazole compound (**6d**) is found to be at the interface between subdomain IIA and IIIA regions as observed from docking results, which is away from the Trp residues, the blueshift of λ_{max} must be due to the moderate conformational changes of BSA in the presence of this compound.

Fluorescence quenching happens with increase in the concentration of ligands by various molecular interactions such as ground-state complex formation, excited state reactions, energy transfer, molecular rearrangement and collision quenching. The quenching process is applicable to understand binding thermodynamics of protein-ligands interactions. The quenching process can be either static or dynamic. Static quenching happens when there is ground-state complex formation between the fluorophore and quencher, and dynamic quenching happens by the collision between fluorophore and quencher at excited states. These two quenching mechanisms can be differentiated by the Stern−Volmer plot using Eq. (1), which also provides the quenching efficiency of oxadiazole compounds on BSA florescence [31].

$$\frac{F_0}{F} = 1 + K_{SV}[Q] = 1 + kq\tau_0[Q] \tag{1}$$

where F_0 and F are the fluorescence intensities of BSA in the absence and presence of oxadiazole compounds, respectively. K_{SV} is the Stern–Volmer quenching constant, τ_0 is the fluorescence lifetime of protein without any quencher, k_q is the

Table 1 Stern–Volmer constant (K_{SV}) and quenching constant (k_q) for the interaction of **6a** and **6d** with BSA at 298, 303 and 308 K

	T (K)	K_{SV} (M^{-1})	k_q (M^{-1} s^{-1})	r^2
	298	7.9×10^3	7.97×10^{11}	0.999
6a	303	5.2×10^3	5.18×10^{11}	0.984
	308	4.6×10^3	4.59×10^{11}	0.987
	298	10.9×10^3	10.90×10^{11}	0.998
6d	303	9.2×10^3	9.16×10^{11}	0.992
	308	7.3×10^3	7.34×10^{11}	0.997

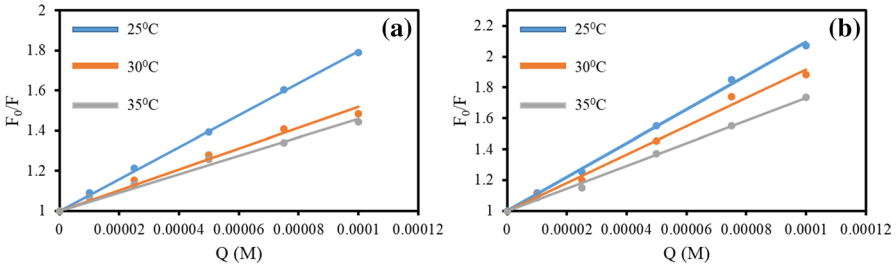

Fig. 4 Fluorescence quenching efficiency of oxadiazole compounds on BSA. Stern–Volmer plots of the fluorescence quenching of BSA by **6a** (**a**) and **6d** (**b**)

bimolecular quenching rate constant and [Q] is the concentration of oxadiazole compounds. The calculated K_{SV} and k_q values for BSA–oxadiazole complexes at different temperatures are presented in Table 1. (Stern–Volmer plots are shown in Fig. 4.) From Table 1, it is observed that calculated K_{SV} values are decreased with increase in temperature. This suggests that the major quenching mechanisim is due to static in nature.

Determination of binding parameters

We used the following equation considering the binding of oxadiazole molecules independently to a set of equivalent sites on BSA to obtain the binding constant (K) and a number of binding sites (n):

$$\log \frac{F_0 - F}{F} = \log K_b + n \log [Q] \tag{2}$$

where n is the number of binding sites and K_b is the binding constant. The values of n and K_b were obtained from the slope and intercept of the plot of log [(F_0−F)/F_0] versus log [Q], respectively (Fig. S2). The calculated results for compounds (**6a** and **6d**) at different temperatures (298, 303 and 308 K) are given in Table 2. The value of n was found to be closer to unity indicating there was one independent class of binding sites on BSA. K_b values for **6a** and **6d** were found to be 1.6×10^3 and 9.0×10^3, respectively, which are in agreement with the docking results where the

Table 2 Binding parameters (binding constant—K_b and binding sites—n) and thermodynamic parameters (Gibbs free energy—ΔG^0, enthalpy—$\Delta H^0$and entropy—ΔS^0) for the interaction of **6a** and **6d** with BSA at 298, 303 and 308 K

	T (K)	K_b (M^{-1})	r^2	n	$-\Delta G^0$ (kJ mol^{-1})	ΔH^0 (kJ mol^{-1})	ΔS^0 (J mol^{-1} K^{-1})
	298	1.6×10^3	0.997	0.86	18.42	−41.59	−77.74
6a	303	1.4×10^3	0.998	0.86	18.03		
	308	0.9×10^3	0.997	0.83	17.65		
	298	9.0×10^3	0.996	0.98	22.56	−40.58	−60.46
6d	303	6.8×10^3	0.987	0.97	22.26		
	308	5.3×10^3	0.982	0.96	21.96		

strongest binding was observed for **6d**. The low values of binding constant reveal that weak interactions exist between oxadiazole compounds and BSA. Generally, protein–ligand complexes exhibit binding constants in the range of 10^5–10^8 $Lmol^{-1}$ [32]. However, there were several reports which show lower binding affinity (10^2–10^4 $Lmol^{-1}$) for several ligand–protein complexes [33, 34]. In one of the studies, binding constant of 2.95×10^3 $Lmol^{-1}$for 1,3,4-oxadiazole compounds of fatty acid with human serum albumin (HSA) was evidenced by Laskar et al. [27]. Another study by Rehman et al. reported binding constants in the range of 1.0×10^4–3.0×10^7 $Lmol^{-1}$ for different 1,3,4-oxadiazole compounds with BSA [35].

Evaluation of thermodynamic parameters and mode of interaction

Several binding forces (viz. electrostatic forces, hydrogen bonding, hydrophobic interactions and van der Waals interactions) are responsible for binding of ligands with biomolecules. Thermodynamic parameters such as enthalpy change (ΔH), entropy change (ΔS) and free energy change (ΔG) can be used to distinguish the type of interaction involved in binding based on the signs and magnitude. The thermodynamic parameters can be obtained from the plot of $\ln K_b$ vs. temperature (Fig. S3) according to the van't Hoff equation as follows:

$$\ln K = -\frac{\Delta H}{RT} + \frac{\Delta S}{R} \tag{3}$$

$$\Delta G = \Delta H - T\Delta S \tag{4}$$

where, K is the equilibrium binding constant (L mol^{-1}), T is the temperature (K) and R is the gas constant (8.314 J mol^{-1} K^{-1}). According to Ross's theory, if $\Delta H > 0$ and $\Delta S > 0$, hydrophobic interactions play a major role; if $\Delta H < 0$ and $\Delta S < 0$, the major binding forces involve hydrogen bonding or van der Waals forces, and if $\Delta H < 0$ and $\Delta S > 0$, electrostatic forces play a major role. The calculated thermodynamic parameters for the interaction of oxadiazole compounds with BSA are given in Table 2. The negative value of ΔG indicates that the interaction is spontaneous and the negative values of ΔH and ΔS suggest that the binding between oxadiazole compounds and BSA is mainly driven by hydrogen bonding and van der Waals forces.

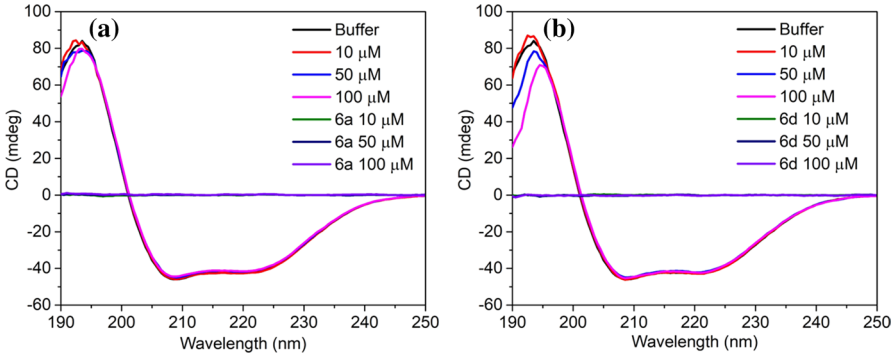

Fig. 5 Secondary structure and conformational stability of the BSA after interaction with oxadiazole compounds. Far-UV CD spectra of BSA in the presence of **6a** (**a**) and **6d** (**b**) with concentrations (0, 10, 50, 100 μM) at 25 °C. Free oxadiazole solutions without protein are represented as **6a** and **6d** followed by concentration

Table 3 α-helix percentage of BSA in the absence and presence of **6a** and **6d**

	0	10 μM	50 μM	100 μM
6a	61.2	60.4	59.1	58.7
6d	61.2	61.1	59.1	59.9

Circular dichroism spectral analysis

CD spectroscopy has been employed to study the changes in the secondary structure of BSA after the interaction with **6a** and **6d**. The secondary structure of BSA exhibits two characteristic negative bands in the far-UV region (190–250 nm). The negative bands at 208 and 222 nm appear due to the π–π* and n–π* transitions of peptide backbone in α-helices. Alterations in the band intensity and position would indicate the conformational changes of BSA after interaction with **6a** and **6d**. Figure **5** shows the secondary structure of BSA in the absence and presence of **6a** and **6d**. It was observed that the structure of BSA remains intact after interaction with **6a** and **6d**. However, to investigate the slight changes induced by the oxadiazole derivatives, we calculate the percentage of α-helix in BSA using Eq. 5:

$$\propto -\text{helix}\ (\%) = \frac{-\text{MRE}_{208} - 4000}{33000 - 4000} \tag{5}$$

where $\text{MRE} = \frac{\text{observed CD}(m\text{deg})}{C_p \text{nl} \times 10}$ [where Cp is the molar concentration of the protein, n is the number of amino acid residues (583 for BSA) and l is the path length (0.1 cm)].

Table 3 shows the percentage of α-helix in the presence of **6a** and **6d**. It was observed that there was a slight decrease in the α-helicity of BSA after interaction with **6a** and **6d** at higher concentration. Conformational changes of serum albumin

in the presence of 1,3,4-oxadiazole compounds with different concentrations were also reported in earlier studies [27].

Esterase-like activity assay

The influence of the oxadiazole compounds on the activity of BSA was monitored using *p*-nitrophenyl acetate (PNPA) substrate. The action of BSA on the substrate was probed by measuring the absorbance of the liberated product, *p*-nitrophenol (λ_{abs} = 400 nm). The catalytic activity of BSA is exhibited by the reactive residues Tyr-411, Lys-413 and 414, which readily react with substrate and acetylated [36]. The activity was provided in terms of units where one unit activity is equal to the amount of enzyme (BSA) required to liberate 1 µM of *p*-nitrophenol from the substrate (PNPA) per minute at 37 °C. For comparative study, BSA activity was represented in relative percentage where the activity of BSA in buffer medium was taken as 100%. Figure 6 shows the relative esterase-like activity of BSA in the presence of **6a** and **6d** with varying concentrations. It is clear from Fig. 6 that the esterase activity of BSA is not much influenced by the oxadiazole compounds. However, with an increase in the concentration of the compounds, there was a slight loss of activity observed, which indicates that BSA maintains the esterase-like activity (≈ 90%) in the presence of both oxadiazole compounds (**6a** and **6d**).

Conclusion

In this work, we have investigated the binding of oxadiazole compounds with BSA and the effect on the structural stability of BSA using different spectroscopic methods including fluorescence, UV-Vis and CD as well as molecular docking studies. Fluorescence results suggested that static quenching is the primary reason for fluorescence quenching of BSA by oxadiazole compounds. The negative value of free energy change elucidated the spontaneous interaction process between BSA and oxadiazole compounds. The negative values of enthalpy and entropy change specified that the hydrogen bonding and van der Waals forces were involved in the

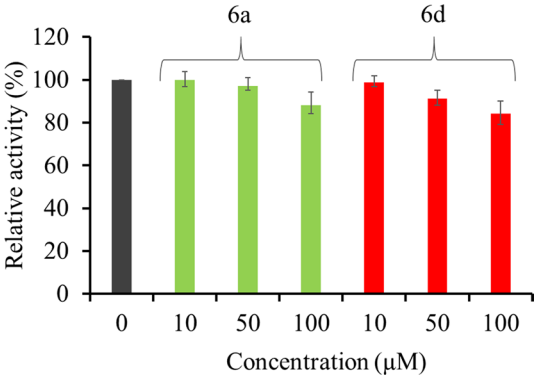

Fig. 6 Modulation in the relative esterase-like activity of BSA as a result of interaction with the oxadiazole compounds (**6a** and **6d**) with concentration (0, 10, 50, 100 µM). (Error bars are found to be less than 6%)

binding of these compounds with BSA which were also supported by the molecular docking results. Moreover, the structural stability of BSA in the presence of these compounds was confirmed by circular dichroism analysis and activity assays. The results showed that BSA remains intact with overall secondary structure after interaction with these compounds retaining ≈ 90% esterase activity. Conclusively, this study presents a comprehensive insight into the possible mechanism of interaction between oxadiazole compounds and BSA that can be helpful for the development of new 1,2,4-oxadiazole compounds.

Acknowledgements The author NPM acknowledges INSPIRE program (DST/INSPIRE/03/2015/004518, New Delhi) for providing financial support in the form of INSPIRE FELLOWSHIP. Author SRM thanks the CSIR, New Delhi, No.-02(0381)/19/EMR-II for financial support.

References

1. A.P. Taylor, R.P. Robinson, Y.M. Fobian, D.C. Blakemore, L.H. Jones, O. Fadeyi, Org. Biomol. Chem. **14**, 6611 (2016)
2. S. Behrouz, M.N. Rad, S. Rostami, M. Behrouz, E. Zarehnezhad, A. Zarehnezhad, Mol. Divers. **18**, 797 (2014)
3. L. Yurttaş, Y. Özkay, H. Karaca Gençer, U. Acar, J. Chem. **2015**, 1 (2015)
4. A. Vaidya, S. Jain, P. Jain, P. Jain, N. Tiwari, R. Jain, R. Jain, A.K. Jain, R.K. Agrawal, Mini Rev. Med. Chem. **16**, 825 (2016)
5. M.A.E. Moneim, J.A. Hasanen, I.M. El-Deen, W.A. El-Fattah, Res. Chem. Intermed. **41**, 3543 (2015)
6. E. Belgodere, R. Bossio, V. Parrini, R. Pepino, Arzneimittelforschung **30**, 1051 (1980)
7. B.O. Buckman, R. Mohan, S. Koovakkat, A. Liang, T. Lan, M.M. Morrissey, Bioorg. Med. Chem. Lett. **8**, 2235 (1998)
8. M. Larif, A. Adad, R. Hmammouchi, A.I. Taghki, A. Soulaymani, A. Elmidaoui, M. Bouachrine, T. Lakhlifi, Arab. J. Chem. **10**, S946 (2017)
9. S. Viveka, Dinesha, P. Shama, G.K. Nagaraja, N. Deepa, M.Y. Sreenivasa, Res. Chem. Intermed. **42**, 2597 (2016)
10. M. Bhat, G.K. Nagaraja, R. Kayarmar, S.V. Raghavendra, K.P. Rajesh, H. Manjunatha, Res. Chem. Intermed. **42**, 7771 (2016)
11. S.A. Kumar, M. Lohani, R. Parthsarthy, Iran J. Pharm. Res. **12**, 319 (2013)
12. N.C. Desai, N. Bhatt, A. Dodiya, T. Karkar, B. Patel, M. Bhat, Res. Chem. Intermed. **42**, 3039 (2016)
13. Z. Zheng, Q. Liu, W. Kim, N. Tharmalingam, B.B. Fuchs, E. Mylonakis, Future Med. Chem. **10**, 283 (2018)
14. S.S. De, M.P. Khambete, M.S. Degani, Bioorg. Med. Chem. Lett. **29**, 1999 (2019)
15. P. Singh, P. Sharma, J. Sharma, A. Upadhyay, N. Kumar, Org. Med. Chem. Lett. **2**, 8 (2012)
16. M. Zareef, R. Iqbal, N.G. De Dominguez, J. Rodrigues, J.H. Zaidi, M. Arfan, C.T. Supuran, J. Enzym. Inhib. Med. Chem. **22**, 301 (2007)
17. R. Iqbal, M. Zareef, S. Ahmed, J.H. Zaidi, M. Arfan, M. Shafique, N.A. Al-Masoudi, J. Chin. Chem. Soc. **53**, 689 (2006)
18. P.R. Kamath, D. Sunil, A.A. Ajees, Res. Chem. Intermed. **42**, 5899 (2016)
19. D. Kumar, S. Sundaree, E.O. Johnson, K. Shah, Bioorg. Med. Chem. Lett. **19**, 4492 (2009)
20. N. Baral, S. Mohapatra, B.P. Raiguru, N.P. Mishra, P. Panda, S. Nayak, S.K. Pandey, P.S. Kumar, C.R. Sahoo, J. Heterocycl. Chem. **56**, 552 (2019)
21. H. Lai, D. Dou, S. Aravapalli, T. Teramoto, G.H. Lushington, T.M. Mwania, K.R. Alliston, D.M. Eichhorn, R. Padmanabhan, W.C. Groutas, Bioorg. Med. Chem. **21**, 102 (2013)
22. M. Schenone, V. Dancik, B.K. Wagner, P.A. Clemons, Nat. Chem. Biol. **9**, 232 (2013)
23. M. Nishijima, J.-W. Chang, C. Yang, G. Fukuhara, T. Mori, Y. Inoue, Res. Chem. Intermed. **39**, 371 (2013)

24. S. Li, H.-p Li, L. Qin, Res. Chem. Intermed. **39**, 1949 (2013)
25. B.B. Jena, L. Satish, C.S. Mahanta, B.R. Swain, H. Sahoo, B.P. Dash, R. Satapathy, Inorg. Chim. Acta. **491**, 52 (2019)
26. L. Satish, S. Millan, V.V. Sasidharan, H. Sahoo, Int. J. Biol. Macromol. **107**, 186 (2018)
27. K. Laskar, P. Alam, R.H. Khan, A. Rauf, Eur. J. Med. Chem. **122**, 72 (2016)
28. E.H. Anouar, M.E. Moustapha, M. Taha, M.H. Geesi, Z.R. Farag, F. Rahim, N.B. Almandil, R.K. Farooq, M. Nawaz, A. Mosaddik, Molecules **24**, 963 (2019)
29. R. Santosh, A. Prabhu, M.K. Selvam, P.M. Krishna, G.K. Nagaraja, P.D. Rekha, Heliyon **5**, 01255 (2019)
30. A. Bujacz, Acta Crystallogr. Sect. D: Biol. Crystallogr. **68**, 1278 (2012)
31. S. Millan, L. Satish, K. Bera, B. Susrisweta, D.V. Singh, H. Sahoo, J. Phys. Chem. B **121**, 1475 (2017)
32. J.S. Mandeville, E. Froehlich, H.A. Tajmir-Riahi, J. Pharm. Biomed. Anal. **49**, 468 (2009)
33. B. Ojha, G. Das, Chem. Phys. Lipids **164**, 144 (2011)
34. T. Zhou, M. Ao, G. Xu, T. Liu, J. Zhang, J. Colloid Interface Sci. **389**, 175 (2013)
35. A. Rehman, J. Iqbal, M.A. Abbasi, S.Z. Siddiqui, H. Khalid, S. Jhaumeer Laulloo, N. Akhtar Virk, S. Rasool, S.A.A. Shah, H.M. Senn, Cogent Chem. **4**, 1472197 (2018)
36. L. Satish, S. Millan, K. Bera, S. Mohapatra, H. Sahoo, New J. Chem. **41**, 10712 (2017)